Monoclonal Antibodies Show That Kinase C Phosphorylation of GAP-43 during Axonogenesis Is Both Spatially and Temporally Restricted In Vivo

Karina F. Meiri,*‡ Lee E. Bickerstaff,* and James E. Schwob‡

Departments of *Pharmacology and ‡Anatomy and Cell Biology, State University of New York Health Science Center, Syracuse, New York 13210

Abstract. To study the role of kinase C phosphorylation in the distribution and function of GAP-43 we have generated a panel of mAbs that distinguish between GAP-43 that has been phosphorylated by kinase C and forms that have not. One class of antibodies, typified by 2G12/C7, reacts with only the phosphorylated form of GAP-43; it recognizes the peptide IQAS(PO_4)FR equivalent to residues 38–43 that includes the single kinase C phosphorylation site at serine [41]. Another, exemplified by 10E8/E7, reacts with both phosphorylated and nonphosphorylated forms. We have used the antibodies to study the distribution of kinase C-phosphorylated GAP-43 during axonogenesis and in the adult nervous system. Two major findings emerge. First, there is a lag between the initiation of axon outgrowth and the phosphorylation of GAP-43 by kinase C. The extent of this lag period varies between the different structures studied. In some cases, e.g., the trigeminal nerve, our result suggest that kinase C phosphorylation may be correlated with proximity of the growing axon to its target. Second, kinase C-phosphorylated GAP-43 is always spatially restricted to the distal axon. It is never seen either proximally or in cell bodies, even those with high levels of GAP-43 protein. This result also implies that GAP-43 is axonally transported in the non-kinase C phosphorylated form. Thus, kinase C phosphorylation of GAP-43 is not required for axon outgrowth or growth cone function per se and may be more related to interactions of the growth cone with its environment.

INTEREST in the so-called "growth-associated" protein GAP-43 arose after observations that its axonal transport is dramatically induced in neurons that are extending axons during either axonogenesis or regeneration after injury (Skene and Willard, 1981*a*; Kalil and Skene, 1986). Because this induction of axonal transport is not normally reinstated in the injured axons of neurons that do not regenerate successfully, such as those in the mammalian CNS, it seems likely that the function of GAP-43 is closely linked to axon growth and regeneration (Skene and Willard, 1981*a*,*b*; Willard et al., 1987; Benowitz and Routtenberg, 1987). This hypothesis is supported by the enrichment of GAP-43 in growth cones (Meiri et al., 1986, 1988; Skene et al., 1986), the structure that is elaborated at the tip of growing axons specifically to perform functions of motility and pathfinding during axonogenesis and regeneration (reviewed by Bray and Hollenbeck, 1989). Within the growth cone, GAP-43 is associated with the membrane skeleton, a structure that links cytoskeletal elements to membrane proteins and which, by analogy with other motile cell types, is likely to be involved in generating and maintaining growth cone morphology (Meiri and Gordon-Weeks, 1990; reviewed by Fox, 1987). At least some of the GAP-43 in the growth cone membrane skeleton is found at areas of the membrane that are tightly attached to the substrate (Meiri and Gordon-Weeks, 1990). Elucidating the functional significance of the subcellular localization of GAP-43 in growth cones would be facilitated if we knew how any interactions of GAP-43 with other membrane skeleton proteins are regulated. Since GAP-43 is a major substrate for endogenous kinase C (Katz et al., 1985; Hyman and Pfenninger, 1987; Van Hoof et al., 1988; Meiri et al., 1988), it therefore seems likely that phosphorylation will be involved in either GAP-43 function or its interactions with other proteins or both. This hypothesis is supported by observations that increased phosphorylation of GAP-43 correlates with exocytosis, depolarization, and treatment of growth cones with NGF (Van Hoof et al., 1989; Dekker et al., 1990; Meiri, K. F., and D. A. Burdick. *Soc. Neurosci. Abstr.* 1989.573), implying that kinase C phosphorylation of GAP-43 could be a component of a common response of growth cones to diverse extracellular stimuli.

We therefore set out to study the regulation of GAP-43 phosphorylation by kinase C in vivo. We first dephosphorylated pure GAP-43 to remove any constitutively phosphorylated sites, before rephosphorylating it with kinase C. We determined the stoichiometry of phosphorylation, sepa-

rated the single tryptic phosphopeptide and directly sequenced it to directly identify the single phosphorylation site at serine[41]. We than generated a panel of mAbs and used the tryptic phosphopeptide to distinguish a class of mAbs, exemplified here by 2G12/C7, that specifically recognize an epitope on GAP-43 that includes phosphoserine[41]. These antibodies bind exclusively to GAP-43 that has been phosphorylated by kinase C and not to the nonphosphorylated form. We also identified another set of mAbs, exemplified here by 10E8/E7, that recognize a configuration present on both phosphorylated and dephosphorylated GAP-43. We used the antibodies to study the regulation of kinase C phosphorylation of GAP-43 in vivo in three different circumstances; during axonogenesis in the embryonic PNS and CNS, during axonogenesis in the adult olfactory system, and finally, in contrast to these two settings, in adult PNS and CNS. During axonogenesis kinase C phosphorylation of GAP-43 is temporally restricted; i.e., there is a lag after the onset of axon outgrowth before kinase C phosphorylation of GAP-43 occurs. The duration of this lag varies depending on the type of neuron examined. These experiments also show that during axonogenesis kinase C phosphorylation of GAP-43 is spatially restricted to distal axons; i.e., it is never found in the cell body or proximal axons, and the length of the proximal axon that remains unstained may be related to the duration of the lag between the beginning of axon outgrowth and the onset of kinase C phosphorylation. In the adult nervous system, kinase C-phosphorylated GAP-43 is widespread but there are differences in its distribution compared with the nonphosphorylated form. Most notably some types of neurons are conspicuous by the relative lack of the phosphorylated form. The results are discussed with reference to the role of kinase C phosphorylation in GAP-43 function during axonogenesis.

Materials and Methods

Determination of the Kinase C Phosphorylation Site

GAP-43 was purified by extracting neonatal (P1-5) rat forebrain membranes with base, followed by reverse-phase HPLC as described by Changelian et al. (1990). This preparation will be referred to as "HPLC-purified GAP-43." Kinase C was purified from the forebrains of adult rats using the method of Wolf et al. (1985). Activity of kinase C-containing fractions, assayed using histone IIIs (Glynn et al., 1985) was 13–20 pmol/min per mg substrate, and the yield was ~10 μg/g brain. HPLC-purified GAP-43 was dephosphorylated by incubation with alkaline phosphatase coupled to agarose beads at a protein:enzyme ratio of 100:1 for 18 h at room temperature in 20 mM Tris, pH 8, and the reaction stopped by centrifugation to separate the beads. Dephosphorylated GAP-43 was then incubated for 10 min with kinase C at a mole ratio of protein/enzyme of 400–800:1 in a reaction mixture containing (final concentrations) 50 mM Tris pH 7.4, 10 mM $MgCl_2$, 1 mM $CaCl_2$, 40 μg/ml phosphatidylserine, and 200 μM γ [^{32}P]ATP (sp. act. 5 Ci/mmol). Quantitation of phosphorylation of GAP-43 used the procedure of Roskoski (1983), and was performed in triplicate. To determine the site phosphorylated by kinase C, HPLC-purified, kinase C-phosphorylated GAP-43 was TCA precipitated and solubilized in 8 M urea and the pH adjusted to 8.2 with 0.1 M ammonium bicarbonate. TPCK trypsin was added at a protein/enzyme ratio of 20:1 for 10 h at 37°C, and the reaction stopped by the addition of TFA to 0.1%. Peptide fragments were separated by reverse-phase HPLC as described by Changelian et al. (1990), and phosphopeptides were identified by Cerenkov counting of the fractions eluting from the HPLC. Samples of tryptic peptides that had eluted from the C4 column were spotted onto PVDF membrane, subjected to Edman degradation, the amino acid composition deduced and quantitated and the PTH-amino acids sequenced using a continuous flow, gas-phase sequencer by Dr. Ray Paxton (Beckman Institute, City of Hope, Duarte, CA) (Shively et al., 1987).

Production and Screening of Hybridomas

HPLC-purified GAP-43 was suspended in PBS pH 7.4 at a concentration of 1 mg/ml and emulsified with RIBI (Immunochemical Research, Hamilton, MT) adjuvant according to manufacturer's directions. Female Balb/C mice received three intraperitoneal immunizations of 100 μg GAP-43 each time and serum-positive mice received a further tail vein injection of 100 μg of GAP-43 suspended in PBS. 4 d later the spleen cells from those mice were fused with NS1 myeloma cells in the presence of polyethylene glycol (Boehringer-Mannheim, Indianapolis, IN) and resulting hybridomas were selected with hypoxanthine-aminopterin-thymidine (HAT), using conventional techniques. The hybridomas were screened for antibody production in three ways: The initial screen was done on dot blots using 0.1 μg pure GAP-43 (phosphorylated and unphosphorylated forms) in each dot. Immunoreactivity was detected with a biotinylated horse-anti-mouse IgG secondary antibody followed by avidin-biotinylated-HRP (ABC method, Vector Laboratories, Burlingame, CA), and visualized with diaminobenzidine (DAB). Hybridomas that were positive on dot blots were further tested on Western blots of 10% SDS-PAGE of P1 rat forebrain homogenates. Those hybridomas that also gave a positive reaction on Western blots were then tested by immunohistochemistry on coronal sections of P1 rat whole heads that had been fixed in 2% paraformaldehyde. Antibodies that were positive on all three screens were subcloned by limiting dilution, and their isotypes determined with specific secondary antibodies. The antibodies in the tissue culture supernatant are at concentrations between 20 and 100 μg specific IgG/ml medium.

Characterization of the mAbs 2G12/c7 and 10E8/E7

(a) Western Blots. The specificity of the mAbs was tested against homogenates from forebrains of P1 rats as follows: Aliquots (50 μg) of P1 forebrain proteins were separated by two dimensional gel electrophoresis essentially as described previously (Meiri et al., 1986), except that the second dimension consisted of 10% SDS minigels (Bio-Rad Laboratories, Richmond, CA). In some cases 0.5 μg of pure GAP-43 that had been phosphorylated with protein kinase C in the presence of radiolabeled ATP (see below) was added to the forebrain homogenate samples before separation in the first (IEF) dimension to identify the spot on the two-dimensional Western blots that corresponds to kinase C-phosphorylated GAP-43. The second dimension gels were either stained with silver as described previously, (Meiri et al., 1986), or alternatively, proteins from the gels were transferred onto Immobilon-P paper (Western blotted) for 1 h at 100 V using a Bio-Rad minitransfer apparatus according to the manufacturer's directions. Immunoreactivity on Western blots was detected using the ABC method and visualized with DAB as above. In the cases where phosphorylated GAP-43 had been added to the samples, radiolabel was detected by subsequent autoradiography of the Western blots using Kodak-XAR film.

(b) Phosphorylated vs. Dephosphorylated GAP-43. The selectivity of the mAbs for the kinase C-phosphorylated form of GAP-43 was assessed on immunoblots as follows: 2 μg of either kinase C-phosphorylated or kinase C phosphorylated and then dephosphorylated GAP-43 were run on 10% SDS minigels, Western blotted onto Immobilon-P paper, incubated with mAbs, and immunoreactivity visualized using the ABC method as described above.

(c) Identification of Immunoreactive Epitopes of GAP-43. Enzymatic digestion of GAP-43 was used to identify the epitopes recognized by the mAbs: aliquots of the peptides that were generated from kinase C phosphorylated GAP-43 by complete proteolysis with trypsin were dotted onto Immobilon-P paper and incubated with mAbs. Immunoreactivity was detected as described above, and immunoreactive peptides were sequenced as described above. In other experiments HPLC-purified GAP-43 was digested with chymotrypsin in 10 mM Tris pH 7.6 at an enzyme/protein ratio of 1:20, or with V8 protease from *Staphylococcus aureus* in 10 mM Tris pH 6.8 at an enzyme/protein ratio of 1:20. The precise details of these digestions appear in the figure legends.

Immunohistochemistry

For both classes of antibodies the optimum conditions for immunohistochemical staining were determined. A variety of fixatives, including Bouin's fluid, freshly prepared paraformaldehyde at concentrations of 2–4% in 0.1 M phosphate buffer, 1% paraformaldehyde-lysine-periodate in phosphate buffer, 100% ethanol, and Carnoy's solution were tested for preservation of

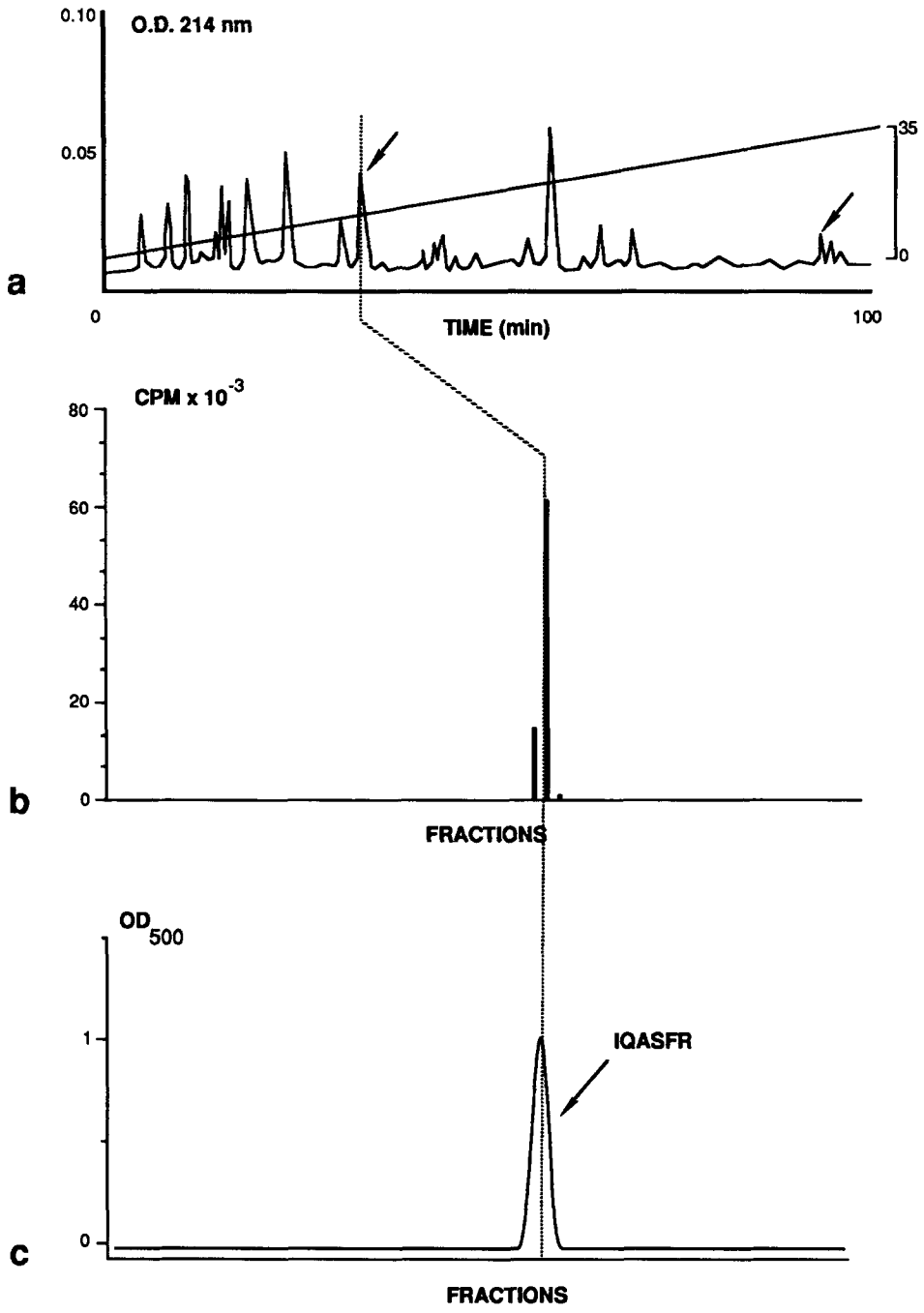

Figure 1. mAb 2G12/C7 reacts specifically with the tryptic peptide containing the kinase C phosphorylation site at serine[41]. (*a*) HPLC separation over a Vydac C4 column of the peptides generated by complete tryptic digestion of 30 μg HPLC-purified GAP-43 that had been dephosphorylated and then rephosphorylated with kinase C. Fractions were collected every minute. *Left ordinate*: optical density monitored at 214 nm of eluted peptides. *Right ordinate*: gradient of 95% acetonitrile in 0.1% trifluoracetic acid used to elute the peptides. The kinase C phosphorylated peptide eluted at 11.4% acetonitrile (*arrow*) and had the sequence IQASFR. (*b*) Cerenkov counts of the tryptic peptides eluted from the C4 column. Only one fraction was radiolabeled (indicated). (*c*) Optical density, monitored at 500 nm, of a dot blot of aliquots of the tryptic peptides that were reacted with the mAb 2G12/C7. Immunoreactivity was detected with the ABC method and visualized with diaminobenzidine. The single immunoreactive dot (indicated) is derived from the fraction containing the phosphorylated tryptic peptide.

immunoreactivity as was unfixed tissue. After fixation tissues were either frozen for cryostat sectioning at 8 μm or embedded in paraffin for sectioning at 5 μm. In general, the patterns of staining were not strikingly different among the various fixatives, although the intensity of the labeling, the sensitivity in demonstrating low levels of staining and the quality of preservation of the labeled elements were affected by the fixative. For 2G12/C7, optimal staining was obtained with tissue that had been fixed in Bouin's solution either by perfusion (in adult or neonatal rats) or immersion (in the case of fetal rats); in both cases total exposure to fixative was limited to 4 h. In the case of the adult rat olfactory epithelium and bulb, the nasal skeleton (after removal of the heavier bones of the skull) was decalcified with either a saturated solution of EDTA, pH 7.0 or with the formic acid-sodium citrate method. Both means of decalcification produced comparable results. Either paraffin or cryostat sections gave excellent results, but maximal sensitivity, i.e., the demonstration of very low levels of staining, was observed with cryostat sections. For example, 2G12/C7-stained individual olfactory axons in the olfactory epithelium were observed only in tissue fixed with Bouin's solution and cryostat sectioned (e.g., Fig. 8 *A*). In contrast, immunostaining of a given structure with 10E8/E7 was best in tissue fixed with periodate-lysine-paraformaldehyde or with low concentrations of paraformaldehyde as compared with Bouin's fixed cryostat sections (although histological preservation was far superior with Bouin's fluid).

After sectioning and mounting, paraffin sections were deparaffinized to water while cryostat sections were rapidly dehydrated to 100% ethanol and then rehydrated to PBS. Subsequent stages in the immunohistochemistry were identical. Nonspecific binding of immunoglobulin was blocked by treating the sections with a 4% BSA/5% nonfat dry milk (NFDM)/10% normal horse serum for 20 min. Subsequently, sections were incubated for 1 h in saturating concentrations of hybridoma supernatants that were diluted in blocking solution with the addition of 0.01% digitonin to improve penetration of the antibody into the section. After washing in 0.5% BSA, tissue-bound antibody was visualized by sequential incubations with biotinylated horse anti-mouse IgG that had been adsorbed to eliminate cross-reactivity with rat tissue (Vector Laboratories, Burlingame, CA) diluted at 1:50 in

blocking solution and with a complex of avidin-biotinylated HRP (Elite kit; Vector Laboratories) in 4% BSA/5% NFDM in PBS used at the recommended dilution. HRP reaction product was developed by incubation in a solution of 0.2% DAB in sodium citrate buffer pH 5.1, and 0.01% H_2O_2 for 7 min.

Results

Identification of the Tryptic Peptide Containing the Phosphorylation Site

The consensus of recent reports is that phosphorylation of GAP-43 by kinase C occurs on serine[41] (Coggins and Zwiers, 1989; Apel et al., 1990). However, a constitutively phosphorylated site would not have been revealed by these analyses, since the native molecule was not dephosphorylated before phosphorylation, nor was the stoichiometry of phosphorylation of native GAP-43 determined in these studies. In fact, GAP-43 has another potential site for kinase C phosphorylation apart from serine[41], namely the serine residue at position 209, which has a carboxy-terminal arginine residue situated as arginine[211] (Edelman et al., 1987; House et al., 1987).

To determine whether both residues are phosphorylated in the intact molecule we purified GAP-43 from neonatal rat forebrains by base extraction followed by reversed-phase HPLC, and then dephosphorylated the pure GAP-43 with alkaline phosphatase to eliminate any constitutively phosphorylated sites before rephosphorylating it with kinase C. When dephosphorylated GAP-43 was used as a substrate, the stoichiometry of phosphorylation was 0.9 mol phosphate/mol GAP-43, compared with 0.7 mol phosphate/mol GAP-43 if HPLC-derived GAP-43 that had not been dephosphorylated was used. This result directly demonstrates that only one serine residue is phosphorylated.

To separate the tryptic phosphopeptide, kinase C-phosphorylated GAP-43 was digested to completion with trypsin, and the resultant peptides separated by reverse-phase chromatography over a C4 column (Fig. 1 *a*); Cerenkov counting revealed only one ^{32}P-containing peptide, which was eluted by 11.4% acetonitrile (Fig. 1 *b*). Edman degradation and amino acid sequencing of this fraction was carried out as described in Materials and Methods. The phosphorylated fraction contained a peptide having the sequence IQASFR, equivalent to GAP-43 residues 38–43, which includes the serine residue at position 41. Computer analysis of the cDNA-derived amino acid sequence of GAP-43 predicted no other tryptic peptide having a serine residue at position 4. By Lineweaver-Burke analysis we calculated that the Km of kinase C for GAP-43 was 5 μM (Fig. 2), which is within the range for GAP-43 to serve as a physiological kinase C substrate (Turner et al., 1985).

Production and Characterization of mAbs

The spleen cell-NS1-myeloma fusions yielded 18 IgG-secreting hybridomas (0.05%) that were positive on dot blots, monospecific for GAP-43 on Western blots of one-dimensional SDS gels, and also stained nervous system tissue specifically using whole head coronal sections from P1 rats. Of these, 13 were further subcloned by limiting dilution. All positive hybridomas gave similar results on the first two screens but could be differentiated into two distinct

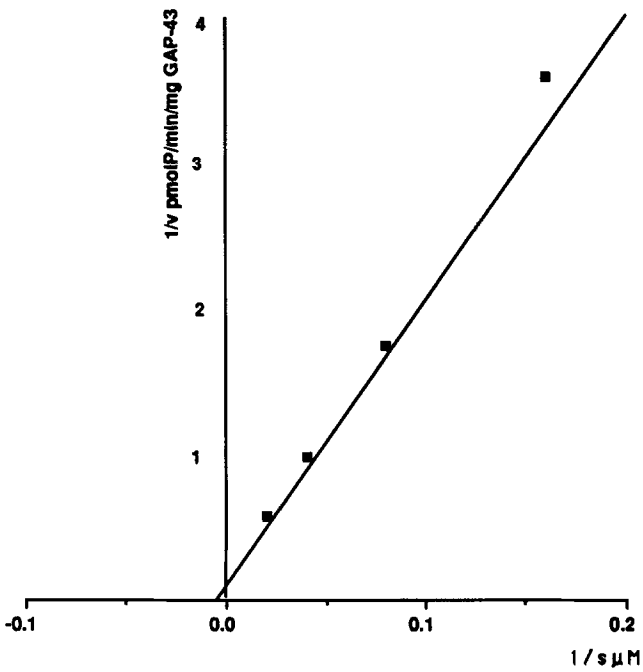

Figure 2. Kinetics of GAP-43 phosphorylation by kinase C Lineweaver-Burke analysis of the phosphorylation of GAP-43 by kinase C. The K_m of kinase C for GAP-43 was calculated to be 5 μM. Each point represents the mean of four determinations.

classes on the basis of their immunoreactivity on tissue sections. This difference in behavior was best exemplified by two antibodies 2G12/C7, an IgG2, and 10E8/E7, an IgG1a, which were investigated further. Additional 2G12-like antibodies included 3D6. Other 10E8-like antibodies included 4E8, 5A6, 5E7, 6C1, 7B10, 8F7, and 10F2.

(a) mAbs 2G12/C7 and 10E8/E7 Are Monospecific for GAP-43, and Discriminate between Different Isoforms. To verify that 2G12/C7 and 10E8/E7 are monospecific for GAP-43, Western blots of two-dimensional IEF gels of P1 rat forebrain proteins were probed with the antibodies. Both 2G12/C7 and 10E8/E7 reacted only with GAP-43 (Figs. 3, *B* and *C*, respectively). However, close examination of these Western blots shows that whereas 2G12/C7 reacts with only the most acidic isoform of GAP-43, 10E8/E7 reacts with all three isoforms (Skene and Virag, 1989), which can be detected after silver staining of the gels (Fig. 3 *A*). The basis for the difference in immunoreactivity was elucidated by mixing protein from neonatal rat forebrain (50 μg/two-dimensional gel) with pure GAP-43 that had been phosphorylated by kinase C in the presence of radiolabeled ATP (0.5 μg/two-dimensional gel), and then separating the mixture by 2D IEF electrophoresis, and Western blotting the second dimension gel. The Western blot that was reacted with 2G12/C7 was subsequently autoradiographed to detect the $\gamma^{32}P$-radiolabeled protein derived from phosphorylation of GAP-43; radiolabel was confined to the isoform recognized by 2G12/C7 (cf. Fig. 3, *C* and *D*).

(b) 2G12/C7 Recognizes Only GAP-43 That Has Been Phosphorylated by Kinase C, Whereas 10E8/E7 Reacts with Both Phosphorylated and Unphosphorylated Forms. To further investigate the restricted nature of 2G12/C7 immunoreactivity, we phosphorylated HPLC-purified GAP-43

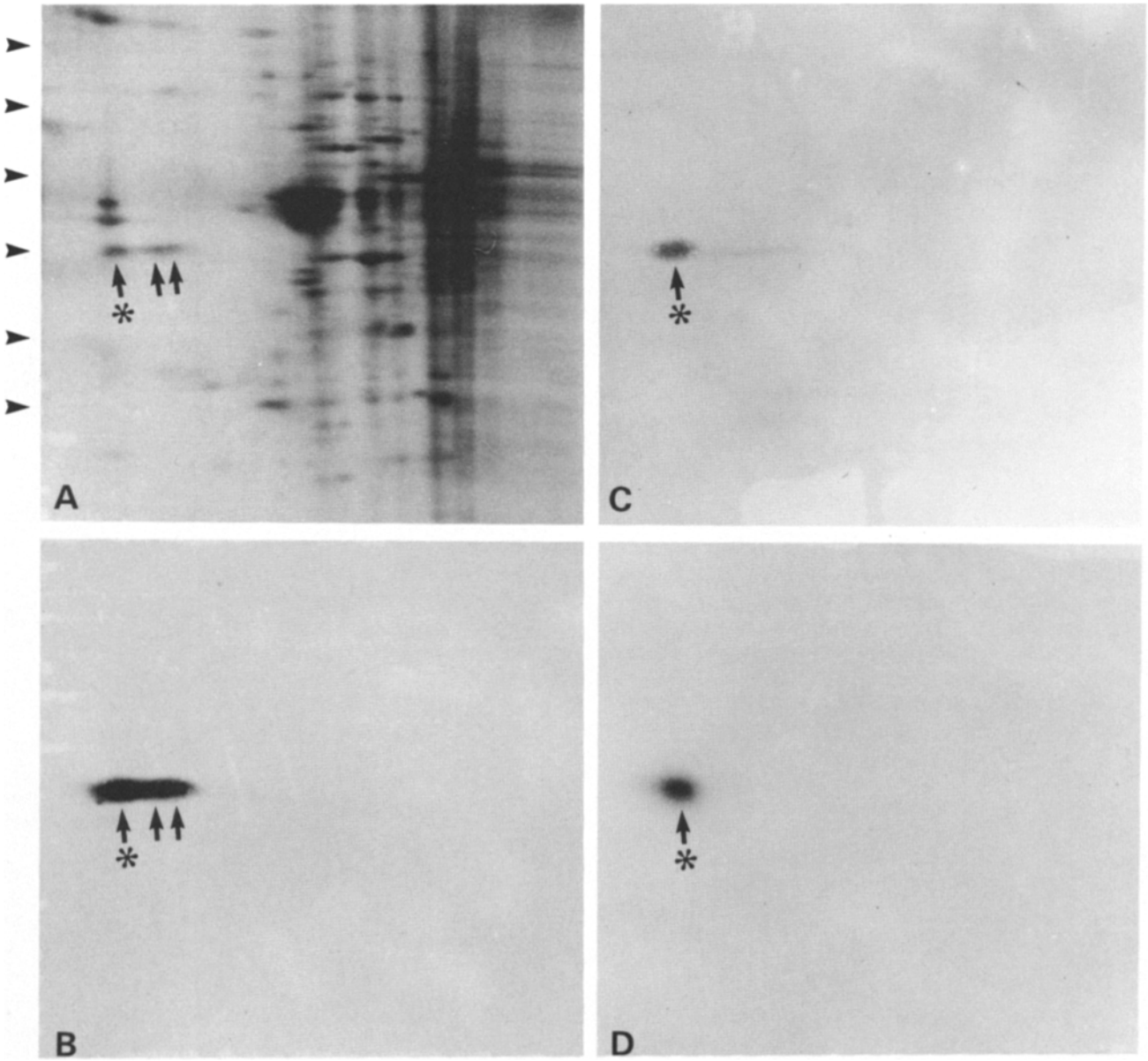

Figure 3. Specificity of the antibodies 2G12/C7 and 10E8/E7. (*A*) Silver-stained gel of P1 rat forebrain proteins (50 μg) that were separated by 2D IEF-PAGE. Proteins were separated in the horizontal (IEF) dimension from pI 4.2 (*left*) to 8.1 (*right*). The second dimension was a 10% SDS gel. The positions of all three isoforms of GAP-43 (pI 4.3–4.7) are arrowed. Note the slanted appearance of the GAP-43 spots. Molecular mass markers indicated by arrowheads are; 180, 116, 97, 58, 48, 36, and 26 kD, from top to bottom. (*B*) Western blot of sister two-dimensional isoelectric focusing gel that was Western blotted and then reacted with 10E8/E7. Immunoreactivity was detected with the ABC method and visualized with diaminobenzidine. The mAb 10E8/E7 is also monospecific for GAP-43 but recognizes all of the isoforms that are detected by silver staining (*arrows*). The starred arrow marks the most acidic isoform. (*C*) Western blot of sister two-dimensional isoelectric focusing gel that was reacted with 2G12/C7. Immunoreactivity was detected and visualized as above. 2G12/C7 is monospecific for GAP-43 and recognizes only the most acidic isoform (*starred arrow*). (*D*) Autoradiograph of two-dimensional isoelectric focusing gel of 50 μg of P1 rat forebrain proteins (as used in *A–C*) to which was added 0.5 μg of HPLC-purified GAP-43 that had been dephosphorylated and then rephosphorylated by kinase C in the presence of γ[^{32}P]ATP. Radiolabel is only detected in the most acidic isoform (*starred arrow*), which is recognized by 2G12/C7.

with kinase C, and then completely dephosphorylated an aliquot with alkaline phosphatase (see Materials and Methods). Both samples were run on 1D gels, Western blotted and immunoreactivity compared. 2G12/C7 only reacted with kinase C-phosphorylated GAP-43 even when the Western blots were heavily overloaded (Fig. 4 *B*). In contrast, 10E8/E7 did not discriminate between phosphorylated and dephosphorylated GAP-43 (Fig. 4 *A*). Interestingly, 2G12/C7, but not 10E8/E7, reacted with proteolytic fragments of GAP-43, (compare Fig. 4 *A*, *left* with Fig. 4 *B*, *left*, and see below). Furthermore, the phosphorylated form of GAP-43 migrates slightly faster than the dephosphorylated form (Fig. 4, *A* and *B*), this finding mirrors the slanted pattern seen on two-dimensional gels (for example Fig. 3 *A*).

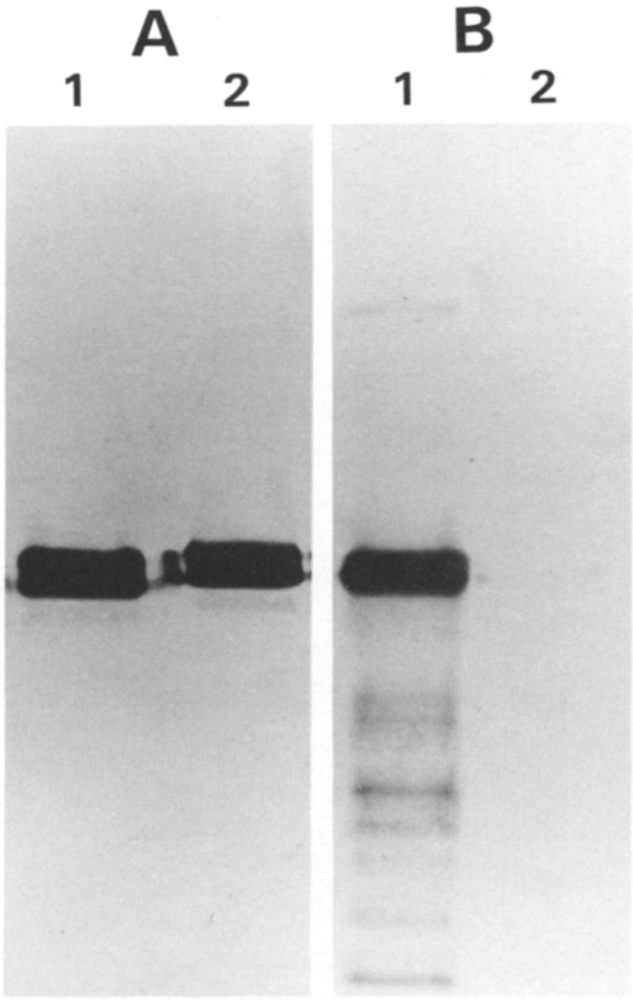

Figure 4. Reactivity of the antibodies with phosphorylated and dephosphorylated GAP-43. (*A*) Western blot of 10 μg of dephosphorylated and rephosphorylated GAP-43 (*left*) versus dephosphorylated GAP-43 (*right*). The blot was reacted with 10E8/E7 and immunoreactivity detected as above. 10E8/E7 reacts with both kinase C-phosphorylated and dephosphorylated GAP-43. Note that phosphorylated GAP-43 runs slightly faster then dephosphorylated GAP-43. (*B*) Similar Western blot of 10 μg dephosphorylated–rephosphorylated GAP-43 and dephosphorylated GAP-43, as seen in *A*, this time reacted with 2G12/C7. Immunoreactivity detected as previously. Note that 2G12/C7 does not react with dephosphorylated GAP-43 even when the blot is severely overloaded, as here. The lower molecular weight immunoreactive proteins are breakdown products (note that 10E8/E7 does not recognize these peptide fragments).

(c) 2G12/C7 Recognizes the Peptide IQA(S-PO$_4$)FR (GAP-43 Residues 38-43), Whereas 10E8/E7 Recognizes an Epitope That Is Destroyed by Even Limited Proteolysis. As we have shown above, of the peptides released by tryptic digestion of kinase C-phosphorylated GAP-43, only a single one contains radiolabeled phosphate (Fig. 1 *b*). Similarly, tryptic digestion of kinase C-phosphorylated GAP-43 was used to identify the portion of the molecule that forms the epitope recognized by the mAb 2G12/C7. When aliquots of all the eluted tryptic fragments were dot blotted onto Immobilon-P paper and reacted with 2G12/C7, immunoreactivity was detected only in the radiolabeled fraction that contained the kinase C-radiolabeled tryptic peptide (Fig. 1, *b* and *c*). Sequence analysis directly confirmed that this radiolabeled, immunostained fraction contains the peptide IQAS(-PO$_4$)FR, corresponding to GAP-43 residues 38–45 and including the kinase C phosphorylation site at serine[41]. Based on these experiments, the epitope of GAP-43 recognized by 2G12/C7 is limited to the phosphorylated form of the tryptic peptide containing the kinase C phosphorylation site.

In contrast, 10E8/E7 immunoreactivity was destroyed by tryptic digestion of GAP-43 even when the digestion was incomplete, and none of the tryptic peptides generated by the digestion were immunoreactive (Fig. 5 *A*). A similar result was obtained when either chymotrypsin or V8 protease from *Staphylococcus aureus* are used to digest GAP-43. In each of these cases too, immunoreactivity with 10E8/E7 disappeared at the onset of proteolysis (Fig. 5). Both chymotrypsin and V8 produce large proteolytic peptides after digestion of GAP-43; chymotrypsin produces two, from residues 1–51, and from 52–239 (Wakim et al., 1987; Changelian et al., 1990), whereas the V8 protease is reported to produce three: 1–63/70, 70–132, and 132–239 (McMaster et al., 1989). Because the proteases cleave at different sites, a fortuitous cleavage by both proteases through the same primary sequence epitope is precluded. Moreover, none of the naturally occurring proteolytic fragments of GAP-43 reacted with 10E8/E7 (compare the right lanes in Figs. 4, *A* and *B*). In contrast 2G12/C7 did react with these proteolytic fragments, further indicating that 2G12/C7 reacts with a primary sequence epitope that is conserved throughout proteolytic degradation. Together, these results suggest that 10E8/E7 may recognize a tertiary epitope, a result that is surprising on two counts: first, GAP-43 has been reported to have little tertiary structure throughout its length. It has a large axial ratio and is apparently composed mainly of random coil (Masure et al., 1986). However, one possibility is that the tertiary epitope may be confined to a particular region in the molecule, such as the NH_2 terminus, where palmitoylation is believed to occur (Skene and Virag, 1989). The sensitivity of 10E8/E7 to fixation conditions is consistent with the notion that the epitope is determined by tertiary configuration rather than primary sequence. If the foregoing is true it is also surprising that 10E8/E7 is immunoreactive on Western blots of SDS gels since this observation suggests that SDS denaturation does not significantly effect the epitope recognized by 10E8. The apparent paradox may possibly be reconciled by the fact that GAP-43 binds less SDS than would have been predicted from its molecular mass (Benowitz et al., 1987), thus making it less subject to denaturation effects.

Immunohistochemical Analysis of the Distribution of Phosphorylated vs. Total GAP-43

Based on the foregoing biochemical analysis, the spatial distribution of the kinase C phosphorylated form of GAP-43 within a neuron can be detected with the monoclonal antibody 2G12/C7. In contrast, the distribution of both phosphorylated and nonphosphorylated forms of GAP-43 is revealed by 10E8/E7. Where there is staining with 10E8/E7 but not with 2G12/C7, we can deduce, by a process of subtraction, that GAP-43 is present as the nonkinase C phosphorylated form. For the purposes of this paper we will abbreviate "non-kinase C phosphorylated form(s) of GAP-43,"

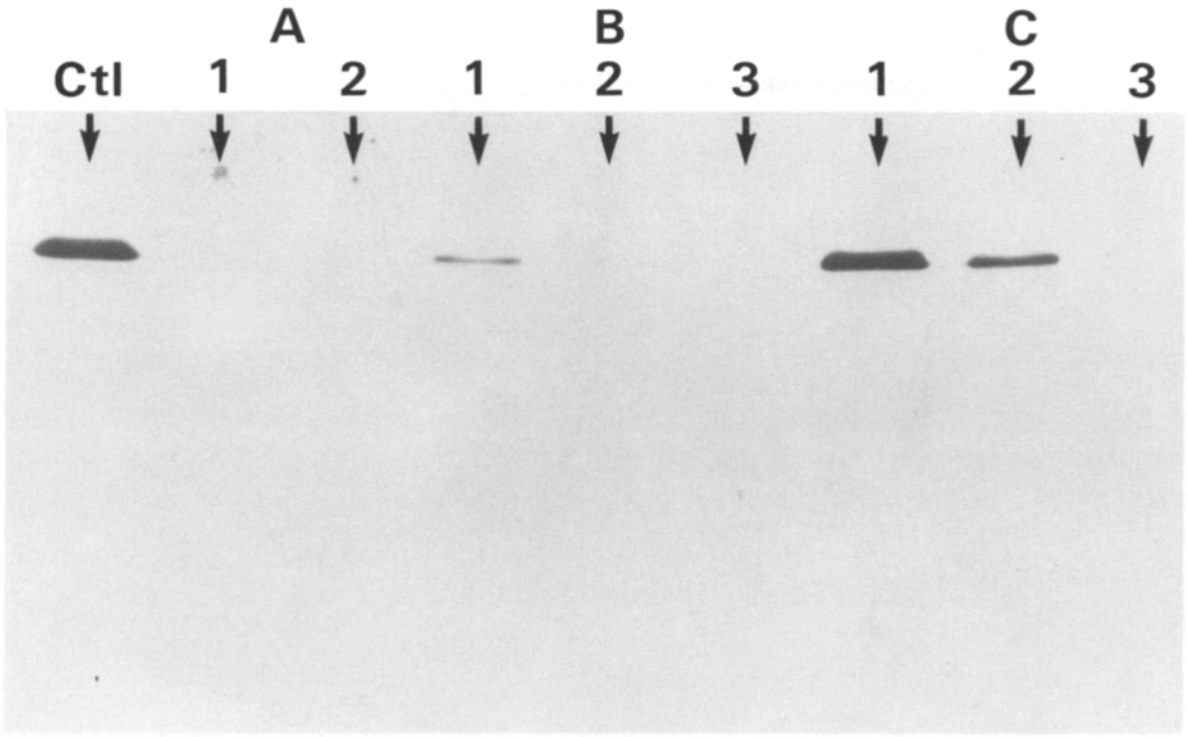

Figure 5. Immunoreactivity with 10E8/E7 is destroyed by even limited proteolysis. Western blot, reacted with 10E8/E7, of 10% SDS gel of pure GAP-43 that had been proteolysed as follows: Ctl; undigested GAP-43 (phosphorylated and dephosphorylated forms). (*A*) Tryptic digestions: (*1*) 1 h, (*2*) 8 h. (*B*) Chymotryptic digestions: (*1*) 1 min, (*2*) 10 min, (*3*) 20 min. (*C*) *Staphylococcus* V8 digestions: (*1*) 10 min, (*2*) 30 min, (*3*) 1 h. Note that in each case immunoreactivity disappears after even limited proteolysis. Each lane contains 1 μg HPLC-purified GAP-43.

which may include form(s) phosphorylated by other kinases such as casein kinase II (Pisano et al., 1988), to "nonphosphorylated GAP-43." We compared the respective distributions of phosphorylated vs. nonphosphorylated forms under several different circumstances. In two of the settings target-directed axonal growth is occurring. First, we examined neurons in the embryonic CNS that have growing axons. Second, we used the adult olfactory epithelium as a source of newly postmitotic neurons that generate an axon in an adult animal. Third, we examined the distribution of immunoreactivity in the mature central and peripheral nervous system. In all cases, the distribution of 2G12/C7 immunoreactivity, i.e., the kinase C phosphorylated form of GAP-43, is different from that of 10E8, indicating that a balance is struck between phosphorylated and nonphosphorylated GAP-43 in the intact animal. In the developing nervous system and in the adult olfactory projection, the patterns of staining with the antibodies are strikingly different both qualitatively, i.e., areas of the nervous system will stain with 10E8 but not 2G12, and quantitatively, i.e., in areas stained by both, the intensity of labeling with 2G12 is markedly less, even under conditions that optimize 2G12 immunoreactivity at the expense of 10E8 (see Materials and Methods). Accordingly, of the GAP-43 present during axonogenesis, that which is protein kinase C-phosphorylated appears subject to complex and dynamic regulation. In the adult animal, the differences between 10E8 and 2G12 immunoreactivity are largely quantitative, i.e., the spatial distribution of staining is similar, and the intensity of the staining differs only slightly for the two antibodies under conditions that optimize 2G12 immunoreactivity. However, in some cases, such as the postganglionic division of the autonomic nervous system, 2G12 immunoreactivity cannot be detected at all in fibers that are stained with 10E8. Therefore, in at least some parts of the adult nervous system, GAP-43 phosphorylation is likely to be subject to dynamic regulation, such as we have observed in the embryo.

In the Embryonic CNS, Staining with 2G12/C7 Appears after the Start of Axonogenesis and Is Limited to the Distal Axon

We compared the distributions of 2G12 vs. 10E8 immunoreactivity in the CNS and PNS of embryos from E11–E20 days of age (we use E0 to designate the time of conception), and in newborn rats. We studied several embryonic structures at multiple time points during their differentiation, including the cranial nerves and ganglia, the spinal cord and spinal nerves, the retina, the olfactory nerve, and the cortical plate, to elucidate the differences in the patterns of labeling. These structures were chosen because the timing of axon outgrowth has been previously determined using other morphological techniques. From the beginning of axon outgrowth immunostaining with 10E8/E7 is found in cell bodies as well as proximal and distal parts of axons, including, in growing axons, the growth cone. In contrast, kinase C phosphorylated GAP-43 is restricted in both time and space relative to the nonphosphorylated form.

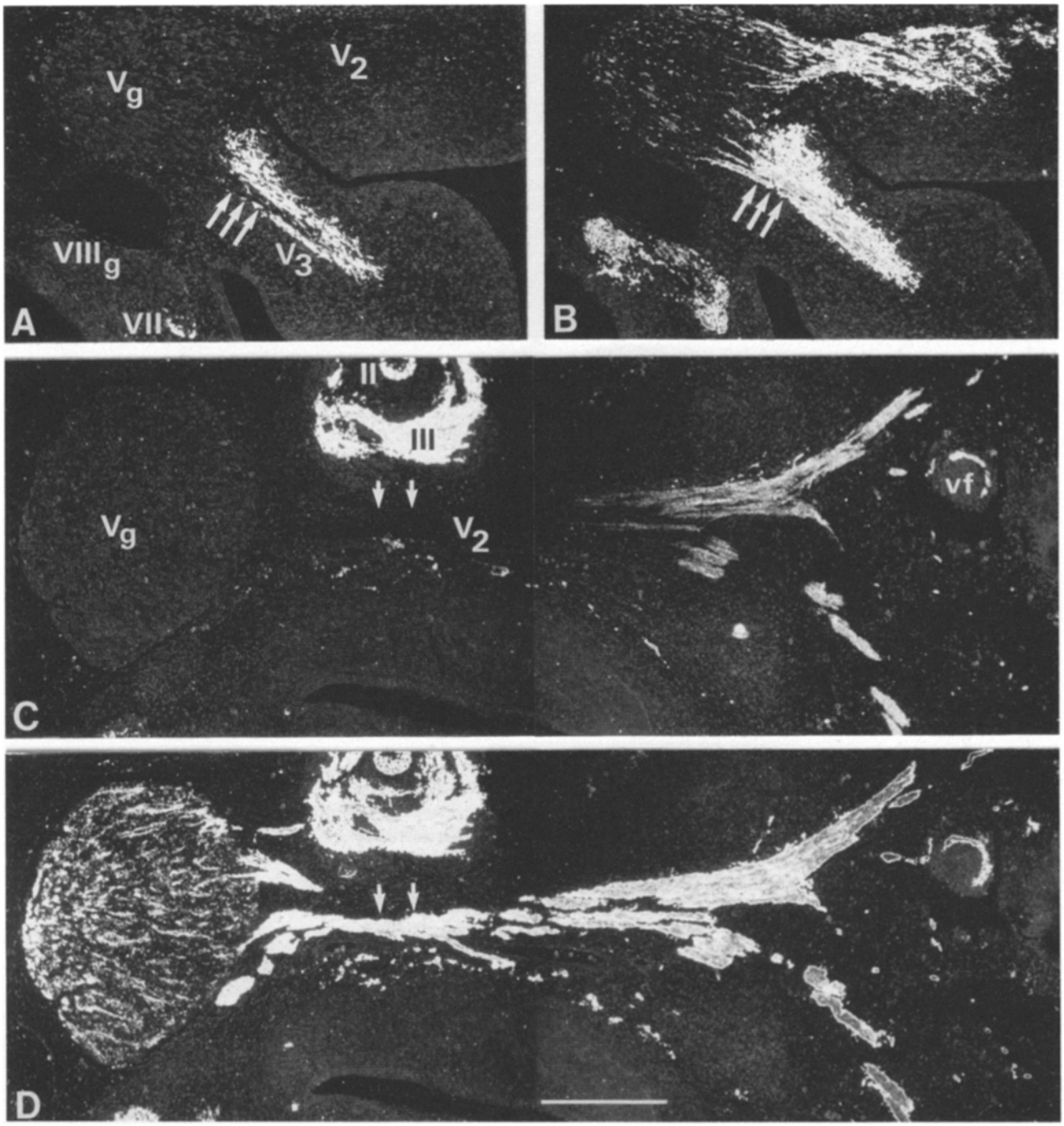

Figure 6. The relative distribution of the kinase C phosphorylated and non-phosphorylated forms of GAP-43 during embryonic development of the trigeminal nerve in rat. (*A*, *B*) darkfield photomicrographs of adjacent parasagittal sections from a Bouin's fixed E12.5 embryo stained with 2G12 and 10E8, respectively. In contrast to their nearly equally intense labeling with 10E8, sensory fibers in both maxillary (V_2) and mandibular (V_3) branches do not stain with 2G12 (*arrows* indicate the unstained sensory fibers in the mandibular nerve). The 2G12 staining in the mandibular branch can be traced to the motor root; therefore, the stained axons are likely to be motor fibers. The illustrated sections were chosen to include the distal extent of both branches. Note the 10E8 labeling and the lack of 2G12 labeling of trigeminal (V_g) and vestibulocochlear ($VIII_g$) ganglia, and the selective labeling of motor fibers of the facial nerve (*VII*). (*C*, *D*) montage of darkfield photomicrographs of adjacent sagittal sections from a Bouin's fixed E15 embryo stained with 2G12 and 10E8, respectively. In the maxillary branch of the trigeminal nerve, 2G12 labeling is confined to its distal part and can be seen in axons that have formed a plexus around a vibrissae follicle (*vf*) as well as the ectoderm (not visible). The length of the proximal nerve that is free of 2G12 labeling roughly corresponds to the length of nerve that was extant at the time when kinase C phosphorylated GAP-43 could be detected distally (cf. length of unstained nerve in *A* and *C*). Bar: (*A*–*D*) 250 μm.

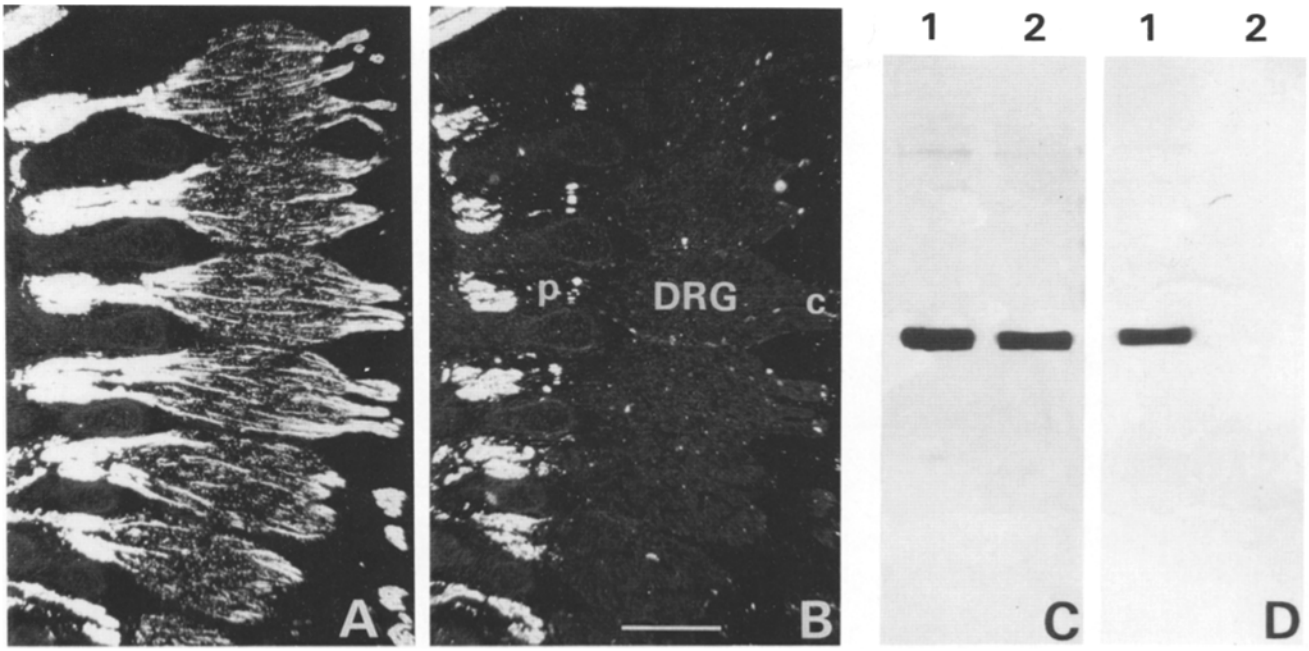

Figure 7. Both immunohistochemistry and Western blotting demonstrate the absence of kinase C-phosphorylated GAP-43 in embryonic dorsal root ganglia (*DRG*) cell bodies and their proximal axons. (*A*, *B*) Darkfield photomicrographs of adjacent parasagittal sections through cervical levels of an E15 embryo (rostral is up): (*A*) stained with 10E8/E7. (*B*) Stained with 2G12/C7. Peripherally directed dorsal root axons are indicated (*p*), whereas centrally directed axons are designated (*c*). (*C*, *D*) Western blots of tissue harvested from embryos of similar age as that illustrated in *A* and *B*. In each case lane *1* contains forebrain proteins while lane *2* contains protein derived from DRG's. Similar amounts of protein (~10 μg) were loaded in each lane. (*C*) Stained with 10E8/E7. (*D*) Stained with 2G12/C7. Bar: (*A* and *B*) 250 μm.

The development of the trigeminal ganglion and nerve illustrates many of the differences between the distribution of the phosphorylated form of GAP-43 vs. the distribution of the nonphosphorylated form. For the trigeminal nerve, these differences are twofold: first, the expression of the phosphorylated form of GAP-43 is delayed relative to the beginning of fiber outgrowth, and the length of the delay differs between motor and sensory fibers. Second, the phosphorylated form of GAP-43, when it does appear, is absent from the proximal axon and cell body and is thereby limited to the more distal part of the growing axon.

At the early stages in the formation of the trigeminal nerve (i.e., E11.75–E12.5), growing motor and sensory axons can be recognized by their staining with 10E8. Indeed, the tips of individual fibers, which we can recognize by also labeling them with antibodies to NCAM (data not shown), stain well with 10E8 suggesting that, in the intact animal, GAP-43 is present in the growth cone, as has been observed in vitro (Meiri et al., 1986, 1988; Skene et al., 1986). There is also weak 10E8-staining of the neuronal cell bodies in the trigeminal ganglion at this time in material that has been prepared to optimize 10E8 immunoreactivity by fixation in either periodate-lysine-paraformaldehyde solution or low concentrations of paraformaldehyde. By E11.9 there is weak 2G12 staining of the motor axons from the level of the brainstem, as they pass ventral to the trigeminal ganglion to the growing front of the mandibular nerve; neither motoneuron cell bodies nor the short intrapontine course of the motor root stain with 2G12. In contrast, at this stage, there is no 2G12 staining of the sensory axons in the mandibular nerve (which can be discriminated from the motor fibers by their continuity with the trigeminal ganglion) nor the maxillary nerve (a purely sensory branch of the trigeminal). By E12.5, as additional axons are recruited into the trigeminal nerve, the contrast between sensory and motor axons with reference to 2G12-staining becomes quite striking. For example, the ophthalmic (also a purely sensory branch), maxillary and mandibular nerves are all prominently labeled with 10E8, indicating that all three consist of a substantial number of axons, yet of the three divisions of the trigeminal nerve only a part of the mandibular branch stains with 2G12 (Fig. 6, *A* vs. *B*). Moreover, the portion of the mandibular nerve that fails to stain well with 2G12 contains sensory axons at high density, as demonstrated by the continuity of 10E8-stained axons from the ganglia into this non-2G12 stained portion of the nerve (Fig. 6 *B*). By E13.5–13.9, the fibers of the maxillary nerve have begun to contact the ectoderm of the muzzle. At this time, the distal parts of the nerve stain weakly with 2G12 in the vicinity of their target, indicating that the phosphorylated form of GAP-43 is now present. The 2G12 labeling of the distal branches of the maxillary nerve continues to increase in intensity over the next few days (Fig. 6, *C* and *D*).

Despite the prominence of 2G12 staining distally in sensory branches at later developmental stages, the proximal part of the sensory fibers, for example where they join the trigeminal ganglion, and neuronal cell bodies in the ganglion remain free of 2G12 immunoreactivity (Fig. 6 *C*). Thus, even after protein kinase C phosphorylation of GAP-43 becomes evident, there is a second, spatial difference in the distribution of the phosphorylated and nonphosphorylated forms of GAP-43. The length of proximal nerve that remains

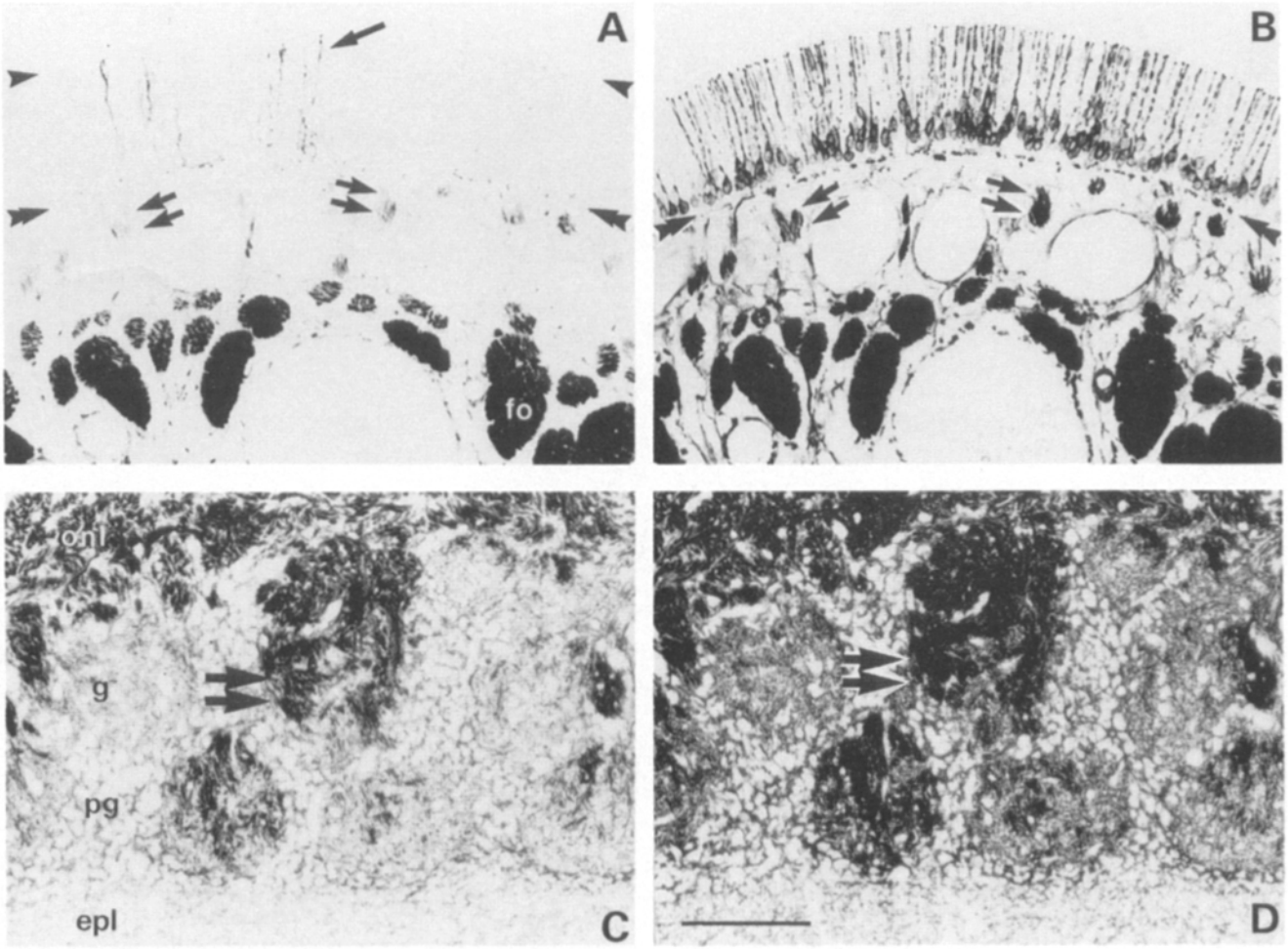

Figure 8. The relative distribution of kinase C-phosphorylated and nonphosphorylated forms of GAP-43 in the adult rat olfactory system. (*A*, *B*) adjacent sections of the olfactory mucosa stained with 2G12 and 10E8, respectively. In the olfactory epithelium (the *single arrowhead* indicates the apical surface and the *double arrowhead* indicates the basal lamina), labeling with 2G12 is limited to the few axons that have been misdirected back into the epithelium (*single arrow*), whereas 10E8 prominently stains a subset of olfactory neurons located just above the zone occupied by basal cells. The fascicles of the olfactory nerve (*of*) situated more superficially in the lamina propria, which contain more proximal segments of olfactory axons, are weakly labeled with 2G12 in some parts and unstained in others. In contrast, there is abundant 10E8 staining of these same fascicles (marked by the *double arrows* in the two sections). The deeper fascicles, which contain axons at a greater distance from their somata, show a more equivalent degree of staining with 10E8 and 2G12. (*C*, *D*) Adjacent sections of the glomerular layer of the olfactory bulb stained with 2G12 and 10E8, respectively. With both 10E8 and 2G12, the intensity of labeling varies in parallel from one glomerulus (*g*) to the next (the *double arrows* mark the same glomerulus in the two sections), although the staining with 10E8 is heavier than that with 2G12, and the variation is due to the different degree of staining of the different groups of olfactory axons that innervate a particular glomerulus. In addition, there is more prominent staining of areas of the olfactory glomerulus that are not associated with olfactory axons in the section labeled with 10E8. Bar: (*D*) 100 μm.

free of 2G12 immunoreactivity correlates with the lag between the onset of axonogenesis and the appearance of phosphorylated GAP-43. This is clearly shown by the contrast between sensory and motor fibers. For trigeminal motor fibers, there is only a brief lag and a correspondingly short length of the motor root that is free of 2G12 immunoreactivity, i.e., motor axons are stained with 2G12 as they exit the brainstem and pass underneath the trigeminal ganglion (data not shown). For sensory fibers, there is a longer lag before 2G12 appears and a correspondingly longer length of proximal axons that remains unstained (Fig. 6 *C*). In other words, GAP-43 that is present in proximal segments of axons is not phosphorylated by protein kinase C (or is not stably phosphorylated) despite the activation of kinase C (or stabilization of phosphorylated GAP-43) in the distal axon.

In all of the other parts of the embryonic nervous system that were examined, the distribution of the phosphorylated form of GAP-43 is likewise restricted both temporally and spatially by comparison with the distribution of the nonphosphorylated forms of GAP-43. These additional observations will not be described in detail here (Schwob, J. E., R. Curtis, G. Wilkins, and K. M. Meiri, manuscript in preparation). However, there are other particularly striking examples of the temporal delay between axon outgrowth and GAP-43 phosphorylation and the resultant limitation of 2G12 immunoreactivity, when it does appear, to the more distal axon.

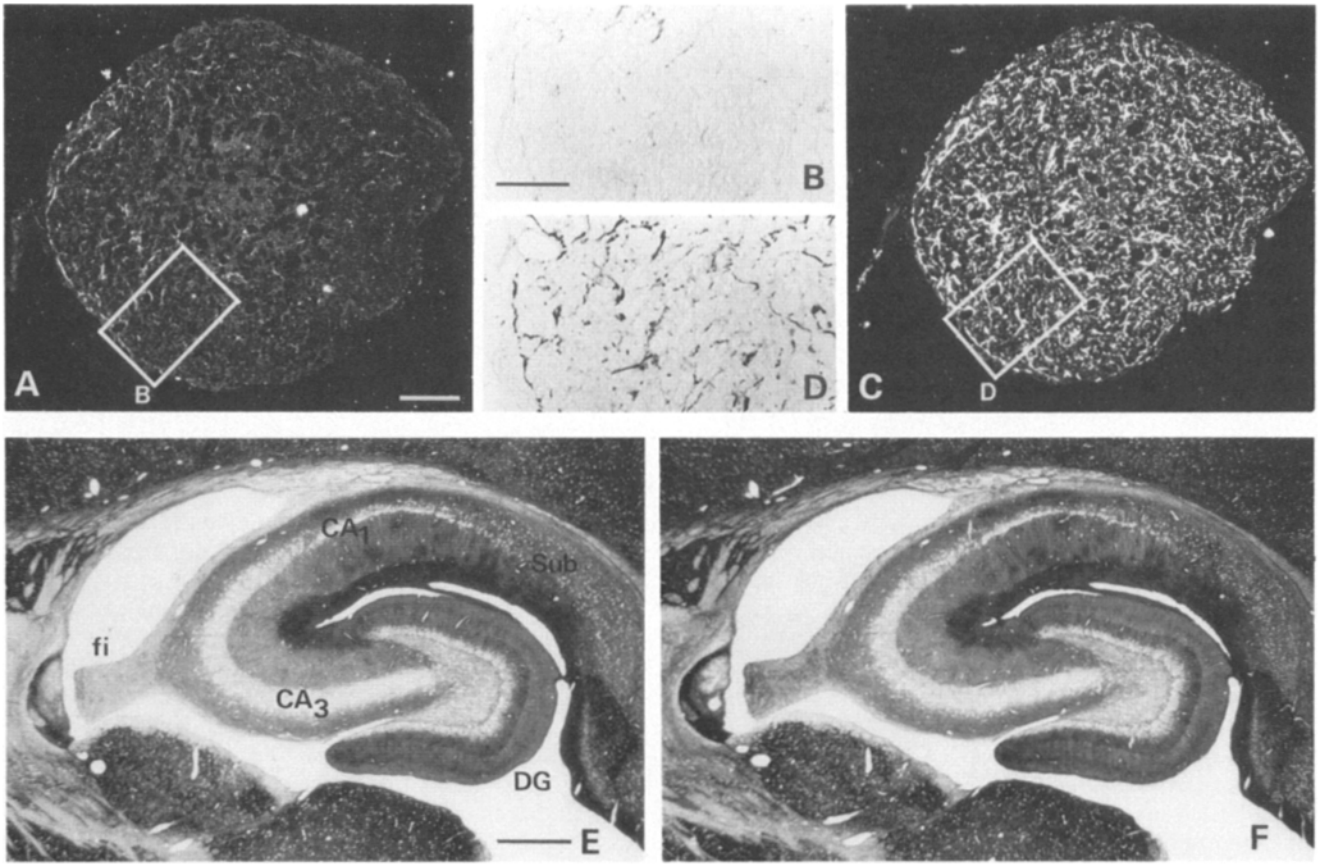

Figure 9. The relative distribution of kinase C phosphorylated and nonphosphorylated forms of GAP-43 in the adult PNS and CNS. (*A*, *C*) Darkfield photomicrographs of adjacent sections of the pineal gland stained with 2G12 and 10E8, respectively. The boxed areas are shown in higher power in *B* and *D*. Note the abundant staining of the nerve plexus with 10E8 as compared with the sparse and weak staining with 2G12. (*E*, *F*) Adjacent sections of the hippocampal formation stained with 2G12 and 10E8, respectively. In contrast to the qualitative differences observed in the pineal gland, there are only slight differences in intensity of staining in fields CA_1 and CA_3 of Ammon's Horn and in the dentate gyrus (*DG*). There is a more substantial difference in staining intensity in the fimbria (*fi*) between the two sections. Bars: (*A*) 250 μm; (*B*) 100 μm; (*E*) 500 μm.

For example, 2G12 immunoreactivity is absent from motor neuron cell bodies in the spinal cord, sensory neuronal cell bodies in the dorsal root ganglia, and growing axons in the anlage of the spinal nerve at the initiation of axonogenesis. When 2G12 immunoreactivity does appear, it is limited to the distal axon and can not be demonstrated in either motoneuron cell bodies, dorsal root ganglia, or proximal axons that were preexisting at the time that 2G12 immunoreactivity becomes demonstrable distally. As for the trigeminal nerve, the lag is longer for sensory fibers than for motor axons.

The observed delay in the onset of 2G12 immunoreactivity and its restriction to distal axons is not an artifact of the immunohistochemical method. We used E15 dorsal root ganglia as an easily isolated source of cell bodies and proximal axons to compare immunohistochemical and biochemical detection methods. In tissue sections, GAP-43 expression in the ganglia is demonstrated by labeling with 10E8, yet 2G12 immunoreactivity is absent (Fig. 7, *A* and *B*). In direct confirmation of these observations, Western blots of dorsal root ganglia were reactive with 10E8 (Fig. 7 *C*), but no immunoreactive band was observed in parallel samples probed with 2G12 (Fig. 7 *D*). These results demonstrate that lack of 2G12 immunoreactivity in tissue sections truly represents absence of the epitope from the dorsal root ganglia cell bodies and proximal axons. In other areas where it is not technically feasible to perform parallel biochemical and immunohistochemical analyses, internal controls, nevertheless, argue for the validity of the observed differences in immunoreactivity between the two antibodies. For example, that differences in 2G12 labeling between proximal and distal axons and between motor and sensory axons are seen in the same section eliminates section-to-section variability. Second, since both 2G12 and 10E8 are IgGs, it is unlikely that differences between the antibodies in their penetration into the section could explain the differences between their distributions. Third, it is unlikely that differential staining with 2G12 merely reflects a lower sensitivity of this antibody relative to 10E8, since decreasing the concentration of 10E8 does not produce a 2G12-like pattern of staining (results not shown). Moreover, if the differences in the staining pattern were solely due to a lower sensitivity of 2G12 rather than an actual difference in the distribution of the epitopes, one would expect that the intensity of 10E8 labeling would predict the level of staining with 2G12. However, 2G12 labeling does not strictly parallel 10E8 staining. For example, in the case of

the trigeminal nerve, the levels of 10E8 staining in mandibular and maxillary branches are roughly equivalent (Fig. 6 *A*), yet there is no 2G12 staining in the sensory fibers of the maxillary nerve (Fig. 6 *B*). Similarly, the dorsal root and dorsal root entry zone at E12–15 is intensely labeled with 10E8 but shows little 2G12 staining, even though other nerves more weakly labeled with 10E8 stain with 2G12 (Fig. 7, *A* vs. *B*). Finally, the spatially and temporally restricted distribution of 2G12 immunoreactivity is observed under all fixation conditions and methods of tissue preparation tested, including unfixed tissue (see Materials and Methods).

In the Primary Olfactory Projection of Adult Rats, Staining with 2G12/C7 Is Limited to the Distal Axon

The olfactory epithelium and its axonal projection to the olfactory bulb (termed here the primary olfactory projection) of adult rats offers the opportunity to study a population of growing axons in adult animals, since progenitor cells in the epithelium constantly give "birth" to neurons that grow an axon through the olfactory nerve toward the CNS (Graziadei and Monti Graziadei, 1979). Therefore, in contrast to the axonal regeneration that occurs in damaged adult peripheral nerves, the newly postmitotic olfactory neurons are an example of axonogenesis in adult animals. As in the embryonic PNS and CNS, the distribution of 2G12 immunoreactivity is more restricted compared with labeling with 10E8. In the epithelium itself, a narrow band of 10E8-stained cell bodies is apparent just above the basal cell layer; the apical dendrites of these neurons also stain with 10E8 and in many cases they extend to the surface of the epithelium where they end in a knob (Fig. 8 *B*). The number of GAP-43-containing olfactory neurons falls as the animal ages, in parallel with the deceleration of growth in neuron number and epithelial surface area as a function of increasing age (Hinds and MacNelly, 1981), but they are found through eighteen months of age at least (the oldest age examined). A similar constellation of findings is observed when polyclonal antisera to GAP-43 are used to label the olfactory epithelium (Verhaagen et al., 1989; Schwob, J. E., unpublished results). Individual 10E8-stained axons can be followed as they descend out of the epithelium and join with small axon bundles just deep to the basal lamina. These small bundles and the larger fascicles of the olfactory nerve are extensively labeled with 10E8, but the staining is nonuniform, indicating that not all of the axons in a fascicle contain GAP-43 (Fig. 8 *B*). The staining pattern with 2G12 is different from that with 10E8 in the olfactory mucosa. In the olfactory mucosa, 2G12 does not label neuronal somata nor the proximal olfactory axons (which are located in the small, most superficial olfactory fascicles in the lamina propria), consistent with its failure to stain cell bodies and proximal axons in the embryonic nervous system (Fig. 8 *A*).

In this context, it is important to note that staining with 2G12 is sufficiently sensitive to label individual olfactory axons in their more distal extent. For example, individual misdirected olfactory axons that reenter the epithelium at a distance from their origin stain with 2G12 (Fig. 8 *B*). Furthermore, the failure of 2G12 to label neuronal somata or proximal axons is found under all conditions of fixation (including unfixed tissue) and is maintained if the proportion of 10E8-labeled olfactory neurons and axons is experimentally induced to increased. For example, after olfactory bulb ablation the vast majority of olfactory neurons, all of which have been generated after the ablation, are morphologically immature and can be stained with 10E8. However, neither cell bodies nor their proximal axons in the small superficial fascicles stain with 2G12 although there is a substantial increase in the staining of the large fascicles, which correspond to the distal parts of olfactory axon, with 2G12 (Schwob, J. E., A. Stasky, and K. E. Szumowski, manuscript in preparation). Therefore, the failure to demonstrate immunoreactivity of proximal olfactory axons and somata is not likely to result from insensitivity of the staining, but rather from the absence (or at the very least a substantially lower amount) of kinase C phosphorylated GAP-43 in the proximal regions of the neuron.

The qualitative differences between the two antibodies in the pattern of labeling of the olfactory epithelium are not evident on examination of more distal olfactory axons. For example, in the distal part of the olfactory nerve near the olfactory bulb and in the olfactory nerve layer around the surface of the bulb, 2G12 and 10E8 label similar portions of the nerve and nerve layer as judged on adjacent sections. In particular, the qualitative equivalence of the staining of distal olfactory axons with the two antibodies is shown best by examining adjacent sections of identified olfactory glomeruli; in every glomerulus that contains GAP-43 immunoreactivity, the region of the glomerulus labeled with 10E8 is also labeled with 2G12. Nonetheless, the intensity of labeling of olfactory axons in glomeruli is always greater with 10E8 (Fig. 8, *C* and *D*). This result demonstrates a quantitative difference in the distributions of the isoforms and indicates that distal olfactory axons contain both the phosphorylated and nonphosphorylated form of GAP-43. In addition to the staining of selected olfactory axons, punctate 10E8 immunoreactivity is also scattered throughout the glomerular neuropil, in parts that do not contain olfactory axons (based on comparison with other markers that label all olfactory axons, such as NCAM; results not shown). In this case, the 10E8 labeling includes a component of nonphosphorylated GAP-43, since there is significantly less staining of the extraolfactory axonal neuropil with 2G12. The location of this nonphosphorylated GAP-43 cannot be identified with certainty at present, but may be found in other types of axons that project into a glomerulus (Price and Powell, 1970).

The difference in the spatial distribution of 10E8 immunoreactivity as compared with 2G12 in the olfactory projection, and specifically the failure of 2G12 to label the proximal olfactory axons in the superficial fascicles of the olfactory nerve in the lamina propria has two implications. First, it indicates that during axonogenesis in the adult olfactory system as in the embryonic nervous system as a whole, kinase C-phosphorylation of GAP-43 is limited to the distal axon and that kinase C does not phosphorylate (or does not stably phosphorylate) GAP-43 present in more proximal axonal segments. Second, the continual generation of new neurons in the olfactory epithelium makes it likely that the tips of the most recently generated axons are present in the superficial olfactory axon fascicles at all times. Hence, the failure to stain superficial axon bundles suggests that the initial stages of axon outgrowth in the adult olfactory epithelium as

in the embryonic nervous system, occur without the elaboration of the phosphorylated form of GAP-43.

The Distribution of Kinase C Phosphorylated GAP-43 in the Adult Nervous System

In contrast to the qualitatively different distribution of the kinase C phosphorylated and nonphosphorylated forms of GAP-43 at the early stages of axonogenesis in the immature nervous system and in the olfactory epithelium, in the adult the differences in the distribution of 2G12 immunoreactivity versus 10E8 immunoreactivity are largely quantitative. However, in several structures, particularly target organs of the postganglionic autonomic nervous system, 2G12 staining is very much reduced or absent relative to staining with 10E8, in contrast to the slight differences in intensity of labeling with the two antibodies that are observed elsewhere. Two examples, namely the pineal gland and the hippocampal formation, may be cited that demonstrate both the differences and the similarities in the distribution of the phosphorylated form (revealed by 2G12) versus both phosphorylated and nonphosphorylated forms (revealed by 10E8) that were found on more extensive examination throughout the whole of the adult nervous system.

The pineal gland is innervated by a plexus of small unmyelinated axons, the vast majority of which are sympathetic fibers derived from the superior cervical ganglia (Kappers, 1976). In the adult rat, 10E8 labels this plexus densely throughout the gland, while 2G12 only weakly stains scattered fibers located near its hilum (cf. Fig. 9, *A* and *B* vs. *C* and *D*). The abundance of 10E8-labeling as compared with the scarcity of 2G12-stained axons indicates that most of the GAP-43 is present in the nonphosphorylated form. A similar preponderance of 10E8 staining relative to 2G12 is generally characteristic of autonomic target tissue in the adult rat, including the sublingual gland, which receives mainly parasympathetic fibers, and the vascular tree. It is worth noting that the phosphorylated form of GAP-43 is relatively abundant during the initial innervation of the pineal gland during embryonic development, when 10E8 and 2G12 labeling are co-extensive, although 10E8 staining of fibers is more intense than that with 2G12 (results not shown).

In the forebrain as a whole and in the hippocampal formation in particular, there is dense staining of the neuropil with both 10E8 and 2G12 (Fig. 9, *E* and *F*). The labeling with 10E8 is slightly more intense than that with 2G12, as shown, for example, by comparing the fimbria on adjacent sections stained with the two antibodies (Fig. 9, *E* and *F*). This result suggests that some of the GAP-43 present in forebrain is nonphosphorylated; however, the relative proportion of the nonphosphorylated to phosphorylated form cannot be easily determined from these experiments, since the tissue was fixed with Bouin's fluid to optimize staining with 2G12 and this means of fixation decreases staining with 10E8. As a consequence, it is likely that the amount of nonphosphorylated GAP-43 has been underestimated by these experiments and that the nonphosphorylated form is a relatively higher proportion of the total pool of GAP-43 than would be indicated by the particular experiments that we have illustrated. Our observations with 10E8 are consistent with previously published descriptions of the distribution of GAP-43-like immunoreactivity in the adult rat forebrain (Benowitz et al., 1988; Oestreicher and Gispen, 1986); for example, in the hippocampus, immunostaining with 10E8 is variably intense across the molecular layer of the dentate gyrus and Ammon's horn, in correspondence with the laminar termination of afferent fibers (Fig. 9 *F*).

Discussion

The data in this paper describe the isolation and characterization of two classes of mAb: one class, exemplified by 10E8, recognizes an epitope present on both protein kinase C phosphorylated and nonphosphorylated forms of GAP-43 that may be a tertiary configuration. The second class of antibodies, exemplified by 2G12/C7, is selective for the kinase C phosphorylated form and binds specifically to a short peptide fragment of GAP-43 that includes phosphoserine[41]. Using 2G12 to localize kinase C phosphorylated GAP-43 and 10E8 to identify both phosphorylated and nonphosphorylated forms, we have shown significant differences between the distribution of the kinase C phosphorylated versus nonphosphorylated form of GAP-43 in the developing nervous system, in the adult primary olfactory projection, which also contains newly postmitotic neurons, and in the adult central and peripheral nervous system.

In differentiating neurons of the embryonic nervous system and the adult olfactory epithelium there is a temporal lag between the beginning of axonal growth and the expression of phosphorylated GAP-43, which is manifested by the absence of 2G12/C7 immunoreactivity from the newly postmitotic, early differentiating neuron; specifically it cannot be demonstrated in axons when they first begin to grow nor in the parent cell body. This lag varies in duration from one type of neuron to another. For example, the delay between the expression of GAP-43 (as shown by labeling with 10E8) and its phosphorylation (as shown by labeling with 2G12) is particularly prolonged in the case of the sensory axons of the trigeminal nerve and the dorsal roots of spinal nerves, but is much shorter in the corresponding motor axons. These results indicate that phosphorylation of GAP-43 is not a requirement for the early stages of axonal outgrowth. An additional indication that axonogenesis occurs independent of kinase C phosphorylation of GAP-43 can be identified even in older animals where phosphorylation occurs more distally. At E14.75 (the age illustrated in Fig. 6 *C*) the proximal maxillary nerve, which is unstained with 2G12, is likely to contain the growing tips of sensory axons, based on the recruitment of axons into the maxillary nerve of the mouse over a four day period after the onset of axonogenesis (Davies and Lumsden, 1984), which would correspond to E11.5 to E16 in rats (based on comparable stages of development).

The fact that kinase C phosphorylation of GAP-43 (or alternatively, the accumulation of phosphorylated GAP-43) is not required for the initial stages of axon outgrowth also suggests that certain growth cone functions are not dependent on phosphorylated GAP-43. One example would be growth cone motility per se since this is presumably ongoing from the initiation of axonogenesis. Membrane addition, which is thought to occur through vesicle fusion (reviewed by Bray and Hollenbeck, 1988), is another aspect of the early stages of axon outgrowth at the growth cone. Our results similarly argue against a role for kinase C phosphorylated GAP-43 in

this type of vesicle fusion in growth cones as had previously been proposed (Gordon-Weeks, 1989).

The second major finding to emerge is the spatial restriction of the phosphorylated form of GAP-43, when it does appear, to the distal axon, so that it is absent from neuronal cell bodies and proximal axons. In particular, kinase C phosphorylated GAP-43 is limited to the tip of the axon in the vicinity of its target in the case of the sensory fibers of the trigeminal nerve.

Our observations on the trigeminal nerve have several implications for the regulation of kinase C phosphorylation of GAP-43. The maintenance of a spatially restricted distribution of kinase C phosphorylation in later embryonic development (i.e., its absence from the proximal sensory branches) indicates that GAP-43 in preexisting axonal segments is not phosphorylated (or is not stably phosphorylated). In turn, this would suggest that kinase C acts on GAP-43 only in regions where membrane is being actively added, such as the distal tip. Additional data on the relative stability and rate of turnover of GAP-43 in growing axons will be required to fully interpret this observation. Furthermore, the absence of 2G12 immunoreactivity from the proximal trigeminal nerve strongly suggests that GAP-43 is being anterogradely transported to the distal end of the axon as the nonphosphorylated form. This interpretation cannot be proven until the lower limit of sensitivity for the immunohistochemical demonstration of the phosphorylated form is determined. Since it has been suggested that the association of GAP-43 with membranes (and hence with transport vesicles) is mediated via fatty acid acylation (Skene and Virag, 1988) these results also imply that acylation can occur independently of phosphorylation.

Given the complex temporal and spatial regulation of kinase C phosphorylation of GAP-43, what may be the mechanism controlling it? The correlation between arrival of sensory axons at the ectoderm (the target field) and the relatively late appearance of 2G12 immunoreactivity in distal axons in the vicinity of the target suggests the possibility that kinase C phosphorylation of GAP-43 is influenced by the target. If this is the case it implies that the lack of phosphorylation seen in cell bodies and proximal axons may not be due to segregation of GAP-43 from kinase C nor from differential distributions of kinase C isoforms, but rather the availability either of competent receptors that are linked to kinase C, or of extracellular stimulators of these receptors. There is some indirect evidence to support this hypothesis. First, there are no morphological data to suggest the segregation of kinase C and GAP-43 in cell bodies; both are present at the cytoplasmic face of the plasma membrane, or associated with vesicles (Saito et al., 1988; Kose et al., 1988; Gorgels et al., 1989; Van Lookeren Campagne et al., 1989), and both are components of the neuronal membrane skeleton (Fernyhough, P., and D. J. Moss. *Soc. Neurosci. Abstr.* 1989. 573; Meiri and Gordon-Weeks, 1990). Furthermore, preliminary evidence of phorbol ester-stimulated phosphorylation of GAP-43 in retinal ganglion cells in vivo (Meiri, unpublished results) indicates that GAP-43 in cell bodies is phosphorylatable by kinase C, provided the kinase is activated. Furthermore, the kinase C-stimulated phosphorylation of GAP-43 in isolated growth cones by physiological concentrations of NGF (Meiri, K. F., and D. A. Burdick. *Soc. Neurosci. Abstr.* 1989.573) shows that GAP-43 phosphorylation can be regulated by target-derived substances. Despite this demonstration of an NGF effect on GAP-43 phosphorylation, we cannot exclude the hypothesis that the onset of kinase C phosphorylation of GAP-43 is intrinsically determined; there is clear precedent for this notion since trigeminal ganglion neurons in mice develop NGF receptors and NGF sensitivity when cultured from a preaxonal stage in the absence of target (Davies and Lumsden, 1984; Davies et al., 1987). In either case, our observations suggest that phosphorylation of GAP-43 is in some fashion required for the interaction of the growing sensory fibers with their target. Taken in total, the findings on differentiating neurons in vivo indicate that phosphorylation of GAP-43 by protein kinase C is under complex spatial and temporal control during axonogenesis.

The findings in adult animals suggest that kinase C phosphorylation of GAP-43 is under complex control in the mature PNS and CNS as well. For example, 2G12 immunoreactive GAP-43 is undetectable in most autonomic fibers in the parenchyma of the pineal gland, despite its abundance during the initial innervation of the gland in the embryo. The significance of the absence of phosphorylated GAP-43 in the pineal gland and its relative prominence in the neuropil of the adult forebrain and hippocampus is unclear at present. However, it may relate to the proposed involvement of kinase C-phosphorylated GAP-43 in the regulation of synaptic function in the adult nervous system (reviewed by Benowitz and Routtenberg, 1987).

In conclusion, the demonstration that GAP-43 phosphorylation may arise as a consequence of such diverse stimuli as treatment with muscarinic agonists, stimulation of exocytosis and membrane depolarization (Dekker et al., 1990; Van Hoof et al., 1989) implies that kinase C activation and resultant kinase C phosphorylation may be a component of a common intracellular response that, in the case of the growth cone, allows it to accommodate different extracellular signals, even though kinase C phosphorylation of GAP-43 is not required for growth cone motility and axon extension per se. Similarly its regulation in the adult nervous system could also reflect a role for GAP-43 in the transduction of extracellular stimuli. These antibodies will enable us to test the hypothesis that regulation of phosphorylation determines the functional state of GAP-43 since we can use them to monitor the kinase C phosphorylation of GAP-43 in situ and the subsequent effects on its interactions with other growth cone proteins.

The authors gratefully acknowledge the expert technical assistance of Audrey Stasky. We also thank Dr. Ray Paxton (City of Hope, Duarte, CA) for sequencing.

This work was supported by NS26091 (K. F. Meiri), DC00467 (J. E. Schwob) and Basil O'Connor Starter Scholar awards from the March of Dimes (K. F. Meiri and J. E. Schwob). J. E. Schwob is an Alfred P. Sloan Research Fellow.

Received for publication 10 August 1990 and in revised form 13 November 1990.

References

Aloyo, V. J., H. Zwiers, and W. H. Gispen. 1983. Phosphorylation B-50 protein by calcium-activated, phospholipid-dependent protein kinase and B-50 protein kinase. *J. Neurochem.* 41:649–653.

Apel, E., M. F. Byford, D. Au., K. A. Walsh, and D. R. Storm. 1990. Identification of the protein kinase C phosphorylation site in neuromodulin. *Biochemistry.* 29:2330–2335.

Benowitz, L. I., and A. Routtenberg. 1987. A membrane phosphoprotein associated with neural development, axonal regeneration, phospholipid metabolism and synaptic plasticity. *Trends Neurosci.* 10:527–532.

Benowitz, L. I., N. I. Perrone Bizzozero, and S. P. Finkelstein. 1987. Molecu-

lar properties of the growth-associated protein GAP-43. *J. Neurochem.* 48:1640–1647.

Benowitz, L. I., P. J. Apostolides, N. Perrone-Bizzozero, S. P. Finkelstein, and H. Zwiers. 1988. Anatomical distribution of the growth-associated protein GAP-43/B-50 in the adult rat brain. *J. Neurosci.* 8:339–352.

Bray, D., and P. J. Hollenbeck. 1988. Growth cone motility and guidance. *Annu. Rev. Cell Biol.* 4:43–61.

Changelian, P., K. F. Meiri, and M. Willard. 1990. Purification of the growth-associated protein GAP-43 by reversed phase chromatography: amino acid sequence analysis and cDNA identification. *Brain Res.* 510:259–268.

Coggins, P. J., and H. Zwiers. 1989. Evidence for a single protein kinase C-mediated phosphorylation site in rat brain protein B-50. *J. Neurochem.* 1895–1901.

Davies, A., and A. Lumsden. 1984. Relation of target encounter and neuronal death to nerve growth factor responsiveness in the developing mouse trigeminal ganglion. *J. Comp. Neurol.* 223:124–137.

Davies, A. M., C. Bandtlow, R. Heumann, S. Korsching, H. Rohreer, and H. Thoenen. 1987. Timing and site of nerve growth factor synthesis in developing skin in relation to innervation and expression of the receptor. *Nature (Lond.).* 326:353–358.

Dekker, L. V., P. N. DeGraan, A. B. Oestreicher, M. DeWit, J. J. Hens, and W. H. Gispen. 1990. Depolarization-induced phosphorylation of the protein kinase C substrate B-50 (GAP-43) in rat cortical synaptosomes. *J. Neurochem.* 54:1645–1652.

Edelman, A. M., D. K. Blumenthal, and E. G. Krebs. 1987. Protein serine/threonine kinases. *Annu. Rev. Biochem.* 56:567–613.

Fox, J. E. B. 1987. The platelet cytoskeleton. *Thromb. Haemostasis.* 175–225.

Gispen, W. H., J. L. M. Leunissen, A. B. Oestreicher, A. J. Verkleij, and H. Zwiers. 1985. Presynaptic localization of B-50 phosphoprotein: The ACTH sensitive protein kinase substrate involved in rat brain polyphosphoinositide metabolism. *Brain Res.* 328:381–385.

Glynn, B., J. Colliton, J. McDermott, and L. A. Witters. 1985. Assay of protein kinase C with a N-bromosuccinimide-cleavage fragment of histone H1. *Biochem. J.* 231:489–492.

Gordon-Weeks, P. R. 1989. The growth cone: what makes it grow? *Trends Neurosci.* 12:238–241.

Gorgels, T. G., M. Van Lookeren Campagne, A. B. Oestreicher, A. A. Gribnau, and W. H. Gispen. 1989. B 50/GAP-43 is localized at the cytoplasmic side of the plasma membrane in developing and adult rat pyramidal tract. *J. Neurosci.* 9:3861–3869.

Graziadei, P. P. C., and G. A. Monti Graziadei. 1979. Neurogenesis and neuron regeneration in the olfactory system of mammals. I. Morphological aspects of differentiation and structural organization of the olfactory sensory neurons. *J. Neurocytol.* 8:1–18.

Hinds, J. W., and A. McNelly. 1981. Aging in the rat olfactory system: correlation of changes in the olfactory epithelium and olfactory bulb. *J. Comp. Neurol.* 302:441–453.

House, C., R. E. H. Wettenhall, and B. E. Kemp. 1987. The influence of basic residues on the substrate specificity of protein kinase C. *J. Biol. Chem.* 262:772–777.

Hyman, C., and K. H. Pfenninger. 1987. Intracellular regulators of neuronal sprouting: II. Phosphorylation reactions in isolated growth cones. *J. Neurosci.* 7:4076–4083.

Kalil, K., and J. H. P. Skene. 1986. Elevated synthesis of an axonally transported protein correlates with axonal outgrowth in normal and injured pyramidal tracts. *J. Neurosci.* 6:2563–2570.

Kappers, J. Ariens. 1976. The mammalian pineal gland, a survey. *Acta Neurochir.* 34:109–149.

Katz, F., L. Ellis, and K. H. Pfenninger. 1985. Nerve growth cones isolated from fetal rat brain III Calcium-dependent protein phosphorylation. *J. Neurosci.* 6:2563–2567.

Kose A., N. Saito, H. Ito, U. Kikkawa, Y. Nishizuka, and C. Tanaka. 1988. Electron microscopic localization of Type I protein kinase C in rat purkinje cells. *J. Neurosci.* 8:4264–4269.

Masure, H. R., K. A. Alexander, B. T. Wakim, and D. R. Storm. 1986. Physicochemical and hydrodynamic characterization of P-57, a neurospecific calmodulin binding protein. *Biochemistry.* 25:7553–7560.

McMaster, D., H. Zwiers, and K. Lederis. 1988. The growth-associated neuronal phosphoprotein B50: improved purification, partial primary structure and characterization and localization of proteolysis products. *Brain Res. Bull.* 21:265–276.

Meiri, K. F., and P. R. Gordon-Weeks. 1990. The growth-associated protein GAP-43 is a component of the growth cone membrane skeleton. *J. Neurosci.* 10:256–265.

Meiri, K. F., K. H. Pfenninger, and M. Willard. 1986. Growth associated protein, GAP-43, a polypeptide that is induced when neurons extend axons, is a component of growth cones and corresponds to pp46 a major polypeptide of a subcellular fraction that is enriched in growth cones. *Proc. Natl. Acad. Sci. USA.* 83:3537–3541.

Meiri, K. F., M. Willard, and M. I. Johnson. 1988. Distribution and phosphorylation of the growth associated protein GAP-43 in regenerating sympathetic neurons in culture. *J. Neurosci.* 8:2571–2581.

Oestreicher, A. B., and W. H. Gispen. 1986. Comparison of the immunocytochemical distribution of the phosphoprotein B-50 in the cerebellum and hippocampus of immature and adult rat brain. *Brain Res.* 375:267–279.

Pisano, M. R., M. G. Hegazy, E. M. Reimann, and L. A. Dokas. 1988. Phosphorylation of protein B-50 (GAP-43) from adult rat brain cortex by casein kinase II. *Biochem. Biophys. Res. Commun.* 155:1207–1212.

Price, J. L., and T. P. S. Powell. 1970. An electron-microscopic study of the termination of the afferent fibers to the olfactory bulb from the cerebral hemisphere. *J. Cell Sci.* 7:157–187.

Roskoski, R., Jr. 1983. Assays of protein kinase. *Methods Enzymol.* 99:3–6.

Saito, N., U. Kikkawa, Y. Nishizuka, and C. Tanaka. 1988. Distribution of Protein kinase C-like immunoreactive neurons in rat brain. *J. Neurosci.* 8:369–383.

Shively, J. E., P. Miller, and M. Ronk. 1987. Microsequence analysis of peptides and proteins. *Anal. Biochem.* 163:517–529.

Skene, J. H. P., and M. Willard. 1981*a*. Axonally transported proteins associated with growth in rabbit central and peripheral nervous system. *J. Cell Biol.* 89:96–103.

Skene, J. H. P., and M. Willard. 1981*b*. Electrophoretic analysis of axonally transported proteins in toad retinal ganglion cells. *J. Neurochem.* 37:79–87.

Skene, J. H. P., and I. Virag. 1989. Posttranslational membrane attachment and dynamic fatty acylation of a neuronal growth cone protein, GAP-43. *J. Cell Biol.* 108:613–624.

Skene, J. H. P., R. D. Jacobson, G. J. Snipes, C. B. MacGuire, J. Norden, and J. A. Freeman. 1986. A protein induced during nerve growth, GAP-43, is a major component of growth cone membranes. *Science (Wash. DC).* 233:783–785.

Turner, R. S., B. E. Kemp, H.-D. Su, and J. F. Kuo. 1985. Substrate specificity of phospholipid/ca dependent protein kinase as probed with synthetic peptide fragments of the bovine myelin basic protein. *J. Biol. Chem.* 260:11503–11507.

Van Hoof, C. O. M., P. N. E. DeGraan, A. B. Oestreicher, and W. H. Gispen. 1988. B-50 phosphorylation and polyphosphoinositide metabolism in nerve growth cone membranes. *J. Neurosci.* 8:1789–1795.

Van Hoof, C. O. M., P. N. E. DeGraan, A. B. Oestreicher, and W. H. Gispen. 1989. Muscarinic receptor activation stimulates B50/GAP-43 phosphorylation in isolated nerve growth cones. *J. Neurosci.* 9:3753–3760.

Van Lookeren Campagne, M., A. B. Oestreicher, P. M. P. van Bergen en Henegouwen, and W. H. Gispen. 1989. Ultrastructural immunocytochemical localization of B-50/GAP 43, a protein kinase C substrate, in isolated presynaptic nerve terminals and nerve growth cones. *J. Neurocytol.* 18: 479–489.

Verhaagen, J., A. B. Ostreicher, W. H. Gispen, and F. L. Margolis. 1989. The expression of the growth associated protein B50/GAP-43 in the olfactory system of neonatal and adult rats. *J. Neurosci.* 9:683–691.

Wakim, B. T., K. A. Alexander, H. R. Masure, B. M. Cimler, D. R. Storm, and K. A. Walsh. 1987. Amino acid sequence of p57 a neurospecific calmodulin binding protein. *Biochemistry.* 26:7466–7470.

Willard, M., K. F. Meiri, and M. I. Johnson. 1987. The role of GAP-43 in axon growth. *In* Axonal Transport, Neurology and Neurobiology. Vol. 25. R. S. Smith and M. S. Bisby, editors. Alan R. Liss, Inc. pp. 407–421.

Wolf, M., P. Cuatrecassas, and N. Sahyoun. 1985. Interaction of protein kinase C with membranes is regulated by Ca2+, phorbol esters and ATP. *J. Biol. Chem.* 260:15718–15722.